OPEN ACCESS
IOP Publishing
Modelling and Simulation in Materials Science and Engineering
Modelling Simul. Mater. Sci. Eng. **30** (2022) 065004 (15pp) https://doi.org/10.1088/1361-651X/ac7ac9

Entropy of kink pair formation on screw dislocations: an accelerated molecular dynamics study

Nikolay Zotov* **and Blazej Grabowski**

Institute for Materials Science, University of Stuttgart, Pfaffenwaldring 55, 70569 Stuttgart, Germany

E-mail: zotov@imw.uni-stuttgart.de

Received 22 February 2022, revised 3 June 2022
Accepted for publication 21 June 2022
Published 30 June 2022

Abstract

The Gibbs energy $\Delta G_{\rm kp}(\tau, T)$ of kink pair formation on screw dislocations in bcc Nb has been determined as a function of shear stress τ at different temperatures $T \leqslant 100$ K using an accelerated molecular dynamics method and a bond-boost potential. From $\Delta G_{\rm kp}(\tau, T)$, the stress dependence of the entropy and the enthalpy of kink pair formation could be obtained using standard thermodynamic relations. The entropy of formation increases with increasing shear stress, following a phenomenologically predicted $\tau^{1/2}$ dependence.

Keywords: accelerated molecular dynamics, bcc Nb, screw dislocations, activation entropy, activation enthalpy

(Some figures may appear in colour only in the online journal)

1. Introduction

It is generally accepted that the motion of screw dislocations in bcc metals at low temperatures takes place by thermally-activated and stress-assisted formation of kink pairs (double kinks) in order to overcome the high Peierls barriers [1, 2]. The thermal activation of kink pairs is a statistical process and their nucleation rate, $J_{\rm kp}$, can be generally written as [3–6]

$$J_{\rm kp} = J_0 \exp\left(-\frac{\Delta G_{\rm kp}(\tau, T)}{k_{\rm B} T}\right), \tag{1}$$

*Author to whom any correspondence should be addressed.

Original content from this work may be used under the terms of the Creative Commons Attribution 4.0 licence. Any further distribution of this work must maintain attribution to the author(s) and the title of the work, journal citation and DOI.

where $\Delta G_{\mathrm{kp}}(\tau, T)$ is the Gibbs energy of formation (activation energy) of a stable (critical) kink pair at a given shear stress τ and temperature T, considered as independent state variables; k_{B} is the Boltzmann constant. The difference between existing rate theories lies in the pre-exponential factor J_0 [3, 7]. A critical kink-pair is defined as a kink pair, the length of which rapidly increases after nucleation, leading to a jump of the dislocation into the next Peierls valley. Thermodynamically, ΔG_{kp} is given by

$$\Delta G_{\mathrm{kp}}(\tau, T) = \Delta H_{\mathrm{kp}}(\tau, T) - T\Delta S_{\mathrm{kp}}(\tau, T), \tag{2}$$

where $\Delta H_{\mathrm{kp}}(\tau, T)$ is the kink pair formation enthalpy (activation enthalpy) and $\Delta S_{\mathrm{kp}}(\tau, T)$ is the kink pair formation entropy (activation entropy). Both, $\Delta H_{\mathrm{kp}}(\tau, T)$ and $\Delta S_{\mathrm{kp}}(\tau, T)$, depend generally on stress *and* temperature. Yet, the temperature dependence of the activation entropy is usually assumed negligible at low temperatures [3]. From the relation $\partial \Delta H_{\mathrm{kp}}/\partial T = T\partial \Delta S_{\mathrm{kp}}/\partial T$, the temperature dependence of the activation enthalpy must be then likewise small. Based on these arguments, it is common to approximate the temperature dependence of the Gibbs energy of formation at *low* temperatures as

$$\Delta G_{\mathrm{kp}}(\tau, T) \approx \Delta H_{\mathrm{kp}}(\tau) - T\Delta S_{\mathrm{kp}}(\tau), \tag{3}$$

where $\Delta H_{\mathrm{kp}}(\tau)$ and $\Delta S_{\mathrm{kp}}(\tau)$ depend only on the shear stress, in contrast to equation (2). Using equation (3), the nucleation rate J_{kp} can be written as

$$J_{\mathrm{kp}} = J_0 \exp\left(\frac{\Delta S_{\mathrm{kp}}(\tau)}{k_{\mathrm{B}}}\right) \cdot \exp\left(-\frac{\Delta H_{\mathrm{kp}}(\tau)}{k_{\mathrm{B}} T}\right). \tag{4}$$

A similar equation is also used for the prediction of dislocation nucleation rates [8].

While the stress dependence of ΔH_{kp} has been discussed in many publications [2, 3, 5, 6, 9–11], very few results on the entropy of kink pair formation exist in the literature. In fact, in many studies the entropy factor, $\exp\left(\Delta S_{\mathrm{kp}}(\tau)/k_{\mathrm{B}}\right)$ in equation (4), is completely neglected or 'absorbed' into the pre-exponential factor J_0.

Several authors approached the problem from a continuum perspective. Specifically, the entropy of thermally-activated dislocation motion has been investigated using the continuum theory of thermo-elasticity at different levels of sophistication [3, 12–14]. For example, the following equation for the activation entropy of dislocation motion, ΔS, was proposed in reference [12]

$$\Delta S = -\frac{1}{\mu}\frac{\partial \mu}{\partial T}\left(\Delta G + \tau V^*\right), \tag{5}$$

where μ is the shear modulus, ΔG the activation Gibbs energy of dislocation motion, and V^* the activation volume. The activation volume is defined such that τV^* is the work done by the external stress [3, 15]

$$V^* = -\left(\frac{\partial \Delta G}{\partial \tau}\right)_T. \tag{6}$$

Equation (5) has, however, the disadvantage that ΔS is an explicit function of the Gibbs energy and thus the stress-dependence appears, in general, in both terms on the right-hand side [16]. Another approach to ΔS was taken by Dimelfi *et al* [13] and later Burns [17], who derived first an equation for the entropy per unit volume s,

$$s(\tau) = \frac{1}{2}\frac{\partial(1/\mu)}{\partial T}\tau^2, \tag{7}$$

which upon integration over the whole volume Ω becomes

$$\Delta S = \int_{\Omega} \Delta s(\tau(V))\mathrm{d}V \tag{8}$$

$$= \frac{1}{2}\frac{\partial(1/\mu)}{\partial T}\int_{\Omega}\left((\tau^*)^2 - \tau_0^2\right)\mathrm{d}V, \tag{9}$$

where τ^* and τ_0 are the shear stresses in the activated and the reference state, respectively. In this approach $\tau^*(V)$ and $\tau_0(V)$ generally depend on volume V, and the resulting entropy increases quadratically with the shear stress. Equation (9) seems attractive for an estimation of ΔS from atomistic simulations, but the actual stress state near the dislocation core is generally more complex than pure shear. Yet another continuum approach was pursued by Kocks *et al* [3] who assumed that the dislocation glide resistance is proportional to the shear modulus μ and with this derived a crude model for the activation Gibbs energy

$$\Delta G = \mu b^3 g(\tau/\mu), \tag{10}$$

from which by definition

$$\Delta S = -\frac{\partial \Delta G}{\partial T} = -\frac{\mathrm{d}(\mu b^3)}{\mathrm{d}T}\, g(\tau/\mu) + \frac{\tau b^3}{\mu}\,\frac{\mathrm{d}g}{\mathrm{d}(\tau/\mu)}\,\frac{\mathrm{d}\mu}{\mathrm{d}T}, \tag{11}$$

where b is the Burgers vector and $g(\tau/\mu)$ an unknown function of τ/μ.

The applicability of these continuum models to the nucleation of kink pairs is generally questionable, because the length of the critical kink pair could be as small as a few Burgers vectors.

Other authors considered a purely atomistic (vibrational) origin of the dislocation entropy and tried to calculate ΔS analytically [18, 19] or numerically [20–23] from the temperature derivative of the vibrational Helmholtz (free) energy

$$\Delta S = -\left(\frac{\partial \Delta F}{\partial T}\right)_{\tau}, \tag{12}$$

where $\Delta F = F^* - F_0$, with F^* the free energy of the activated state and F_0 the free energy of the reference state. The free energy was specifically computed in the harmonic approximation. The phonon frequencies in this approximation are determined numerically by diagonalization of the $3N \times 3N$ dynamical matrix ($N =$ number of atoms), which explains why the approach has been applied only to model systems with relatively small numbers of atoms (typically $N = 75$–2000). However, realistic atomistic calculations of dislocation properties require much larger supercells due to their long-range stress fields. Knowing the phonon frequencies in the ground state (ν) and in the activated state (ν^*), the entropy factor can also be calculated directly using transition state theory [24, 25] as

$$\exp\left(\frac{\Delta S}{k_{\mathrm{B}}}\right) = \frac{1}{\nu_0}\frac{\prod_i \nu_i}{\prod_j \nu_j^*}, \tag{13}$$

where $i = 1, 2, \ldots, 3N$ and $j = 1, 2, \ldots, 3N - 1$ and ν_0 is the attempt frequency. In the case of screw dislocation mobility, the activated state corresponds to the formation of a critical kink pair at a given external critical stress. Consequently, the phonon frequencies of the system must be known as a function of the external stress. Jin *et al* [26] used a stochastic approach to estimate the activation entropy of kink migration on a 30° partial dislocation in Si from equation (13).

To the best of our knowledge, this method has not been applied yet to dislocations in fcc or bcc metals.

The entropic impact on dislocation migration can also be investigated explicitly with molecular dynamics (MD) simulations. A key challenge in such simulations, on top of finite-size restrictions as for the calculation of the phonon frequencies, is the accessible time scale. Several enhanced sampling methods (umbrella sampling, metadynamics, adaptive strain-boost MD and partial-path transition interface sampling) have been applied to estimate entropic effects and the activation volume during dislocation nucleation and creep in fcc and hcp metals as well as diffusion in metallic glasses [8, 27–33]. However, these sampling methods cannot be straightforwardly adapted to the double-kink driven dislocation migration in bcc metals at low temperatures, and thus corresponding investigations are not available.

In the present study, we address the above-discussed simulation challenges by utilizing a recently proposed method for the calculation of the Gibbs energy of kink pair formation [7]. The method gives direct access to the stress *and* temperature dependence of $\Delta G_{\mathrm{kp}}(\tau, T)$ via the general relation of equation (1). It makes use of accelerated MD and overcomes the time-scale problem of atomistic dislocation migration simulations by facilitating the double-kink driven dislocation motion at experimental stresses. Utilizing the method, we determine the entropy ΔS_{kp} for a large system size ($N = 48\,000$), as compared to previous studies, by standard thermodynamic relations. We choose bcc Nb as a prototype system, because Nb has the lowest experimental enthalpy of critical kink pair formation of all bcc transition metals [2].

2. Computational details

The simulations were performed with the LAMMPS package [34] utilizing the embedded-atom method potential of Farkas and Jones [35], which had been thoroughly validated in reference [36]. A dipole model with two (initially) straight screw dislocations with opposite Burgers vectors, both at 'easy-core' positions, was employed (see figure 1). The model was generated using the ATOMSK program [37]. The crystallographic directions along the supercell axes were $X \parallel [01\bar{1}]$, $Y \parallel [111]$ and $Z \parallel [2\bar{1}\bar{1}]$, corresponding to the $(2\bar{1}\bar{1})$ maximum resolved shear stress plane. The screw dislocations were aligned parallel to the Y axis. Periodic boundary conditions were imposed along all three directions X, Y and Z, thus allowing us to model an infinitely long screw dislocation.

The simulation supercell was chosen to have a size of $L_x = 187$ Å, $L_y = 10b = 28.6$ Å and $L_z = 162$ Å, where b is the length of the Burgers vector, equal to 2.86 Å for bcc Nb. The resulting number of atoms in the simulation cell amounted to 48 000. The L_x and L_z values were selected to be the minimum lengths for which the forces between the two screw dislocations along X and the image forces along Z are less than 0.005 eV Å^{-2} (per unit dislocation length). To determine an appropriate L_y value, we performed MD simulations of the dislocation velocity v_{d} at the relevant temperatures (50, 75, 100 K) using dipole models with supercell sizes from $5b$ to $40b$ along the dislocation line. (Due to the periodic boundary conditions, any simulation cell contains an infinite dislocation line; however, finite size effects due to periodic boundary conditions require explicit tests.) The respective results show that v_{d} is, within error limits, independent of the (explicit) dislocation length in the investigated range. Accordingly, the nucleation rate of critical kink pairs, commonly written as $J_{\mathrm{kp}}(\tau, T) = v_{\mathrm{d}}/h$, where h is the height of the KP [38], is in first approximation also independent of the (explicit) dislocation length for the used simulation setup. Based on these tests, the size of the simulation supercell along the Y axis was set equal to $10b$, in order to be able to perform the necessary, large number of MD and hyperdynamics (HD) simulations within reasonable computational times.

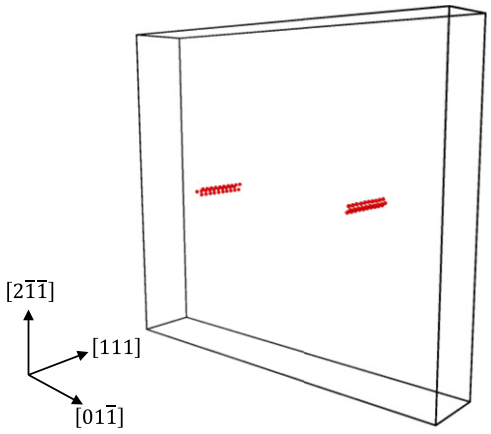

Figure 1. Orientation of the dipole supercell. The core atoms of the two screw dislocations, parallel to [111], are shown in red.

To generate the strain-reduced simulation setup [7], a constant shear along the Y axis was applied to the simulation cell at several temperatures (50, 75 and 100 K; shear strain rate 1×10^8 s^{-1}). Using different initial velocity distributions, the average critical strain $\bar{\gamma}_c$ and average critical stress $\bar{\tau}_c$ (corresponding to an average critical time $\bar{t}_c$), at which one of the screw dislocations starts to move, were determined at each temperature. Afterward, new simulations at several constant reduced shear strains $\gamma_{red} < \bar{\gamma}_c$ were performed at each temperature under *NVE* conditions in order to determine the average waiting time $\langle \Delta t_w \rangle$ for the occurrence of the first jump of one of the screw dislocations. Detailed atomistic analysis of the MD configurations using the coordination neighbor analysis, implemented in the OVITO program [39], showed previously [7] that the first jump takes place by nucleation and growth of a critical kink pair on one of the screw dislocations. The geometry of a critical kink pair is shown in figure 2.

The average waiting time $\langle \Delta t_w \rangle$ increases rapidly with increasing strain reduction (i.e., decreasing constant shear stress τ_{red}). In order to extend the accessible range of shear stresses, the method [7] uses HD [40] and a global bond-boost potential ΔV_b, defined as

$$\Delta V_b = \begin{cases} V_{max}\left(1 - \dfrac{\varepsilon_{max}}{q}\right)^2 & \varepsilon_{max} < q, \\ 0 & \varepsilon_{max} \geqslant q \end{cases} \tag{14}$$

where V_{max} is the magnitude of the boost potential, ε_{max} is the maximum bond strain at a given MD step, i.e., $\varepsilon_{max} = \max_\alpha\{\varepsilon_\alpha\}$, where $\varepsilon_\alpha = \|b_\alpha - b_\alpha^0\|/b_\alpha^0$, b_α is the instantaneous value of bond α, b_α^0 is the initial value of bond α in the boosted region, and q is a threshold parameter. The boost factor BF_i at each MD step t_i is defined as

$$\mathrm{BF}_i = \exp[\Delta V_b(t_i)/k_B T] \tag{15}$$

and the accelerated time of the HD (t_{hyp}) is given by

$$t_{hyp} = \Delta t_{MD} \sum_i \mathrm{BF}_i, \tag{16}$$

where the sum is over the performed MD integration steps and Δt_{MD} is the MD integration time step (1 fs in the present case). The boosted region consists of the dislocation cores of

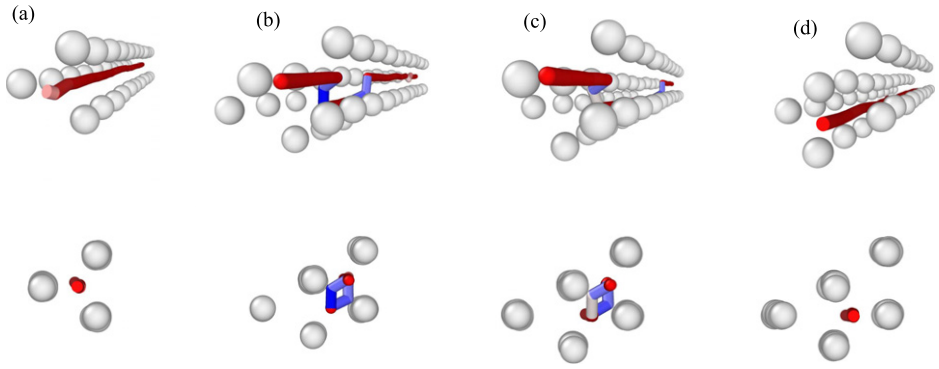

Figure 2. Double-kink nucleation and growth at 75 K and 0.4 GPa. (a) Straight screw dislocation at an easy core position, observed at a time step of 86.70 ps. Only the core atoms (in gray), as determined with OVITO, are shown. The core is non-planar and comprises 30 atoms. (b) A just-nucleated, critical kink pair at a time step of 86.75 ps. The length of the KP is ≈4.0 Å (1.4b) and its height ≈1.6 Å (0.6b). The formation of the KP involves only 5–6 additional (new) core atoms, corresponding to about $4b^3$. The kinks (in blue) are along the $(\bar{1}01)$ and $(0\bar{1}1)$ planes at 30° and 90° to the glide plane, respectively. The effective orientation of the KP is along the $(\bar{1}\bar{1}2)$ plane, at 60° to the $(2\bar{1}\bar{1})$ glide plane. (c) The expanding KP has reached a length of about ≈14 Å (5b) at a time step of 87.55 ps. (d) The screw dislocation has jumped at a time step of 87.85 ps to the neighboring hard core position, at which the core is comprised of 50 atoms. The lower panels are projections perpendicular to the [111] direction. The screw dislocation line is shown in red.

Table 1. Computed critical shear stresses τ_c and optimized bond-boost parameters q and V_{max} for the investigated temperatures T. The estimated standard deviations in τ_c are given in brackets.

T (K)	τ_c (GPa)	q	V_{max} (eV)
50	0.55(3)	0.07	0.01125
75	0.41(2)	0.09	0.025
100	0.29(6)	0.1012	0.031

the two dislocations. The boost potential was applied until a critical kink pair forms on one of the screw dislocations. Temperature equilibration during the HD runs was achieved using a Langevin thermostat with a carefully chosen damping factor. At least 50 HD runs with different initial velocity distributions were performed at each stress level and temperature for sufficient statistical averaging. The boost parameters q and V_{max} were determined at each temperature (see table 1) for a few small strain-reduction levels from the requirement that the average hypertime $\langle t_{hyp} \rangle$ is equal (within statistical errors) to the average waiting time without boosting, $\langle t_{hyp} \rangle = \langle \Delta t_w \rangle$ (see reference [7] for details). These values were then used in all other HD runs at a given temperature.

The critical shear stress decreases with increasing temperature [41]. Thus, the range of shear stresses in the thermally-activated regime, accessible with the above-described strain-reduction procedure, also decreases with increasing temperature. In addition, the boost factor decreases exponentially with increasing temperature (equation (15)), leading to a decrease of the computational speedup of the HD method. In order to maximize the effect of the strain-reduced HD

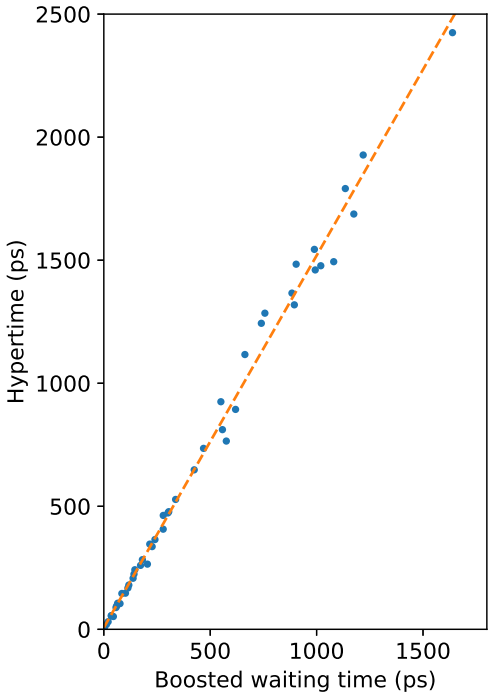

Figure 3. Hypertime versus the boosted waiting time for 48% strain reduction at 100 K. The dashed line is a linear fit yielding an average boost factor of 1.51 ± 0.02.

simulations, the temperature should be as low as possible. However, for bcc Nb, the Arrhenius rate equation (equation (4)) is not valid below ≈50 K [41]. These are the reasons why the present HD simulations were performed in the range 50–100 K.

The individual hypertimes, plotted as a function of the boosted waiting times, show very little scatter (see an example in figure 3). This indicates that the boost potential (equation (14)) is well sampled and the boost parameters, given in table 1, are properly selected [42]. The accelerated MD method leads to average boost factors in the range of 1.2–2.4, depending on the stress level and temperature.

Knowledge of the average hypertimes at different temperatures and constant shear stresses τ ($=\tau_{\rm red}$), provides access to the Gibbs energy of kink pair formation via [7]

$$\Delta G_{\rm kp}(\tau, T) = -k_{\rm B}T \ln\left(\frac{\sigma(\bar{t}_{\rm c})}{\langle t_{\rm hyp}\rangle}\right), \tag{17}$$

where $\sigma(\bar{t}_{\rm c})$ is the estimated standard deviation of the critical time $\bar{t}_{\rm c}$ at the corresponding temperature.

3. Results and discussion

The stress-dependence of $\Delta G_{\rm kp}$ at the three investigated temperatures (50, 75 and 100 K), determined using equation (17), is shown in figure 4 by the symbols. The estimated standard deviations in $\Delta G_{\rm kp}$ increase with increasing temperature due to enhanced thermal vibrations.

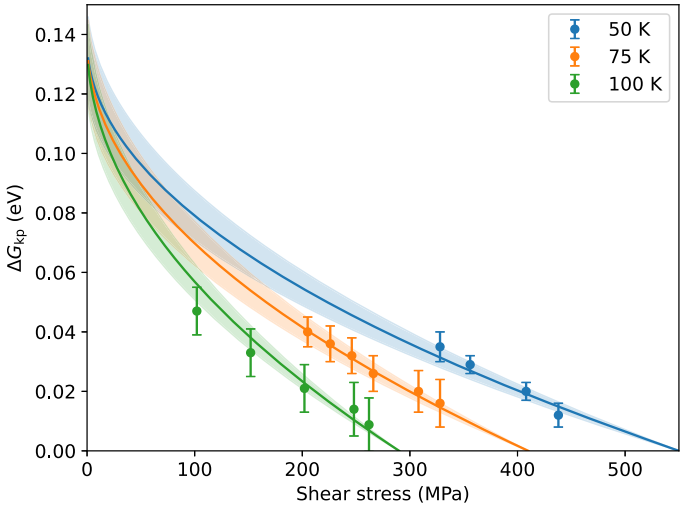

Figure 4. Gibbs energy of kink pair formation as a function of shear stress at different temperatures. The full lines represent the fit of the data using equation (18) (see text for details). The light shaded regions indicate the 95% confidence interval of the fit.

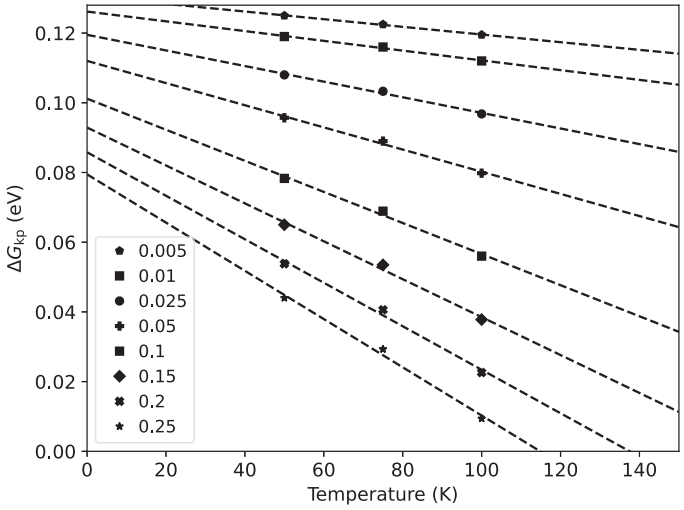

Figure 5. Gibbs energy of kink pair formation as a function of temperature at different stress levels as indicated in the legend in units of GPa. The dashed lines are fits through the data using equation (3).

Using the accelerated MD methodology, it was possible to determine ΔG_{kp} at each temperature to at least 40% strain reduction (40% at 50 K, 50% at 75 K and 65% at 100 K). The activation energies of kink pair formation increase with decreasing shear stress and decreasing temperature.

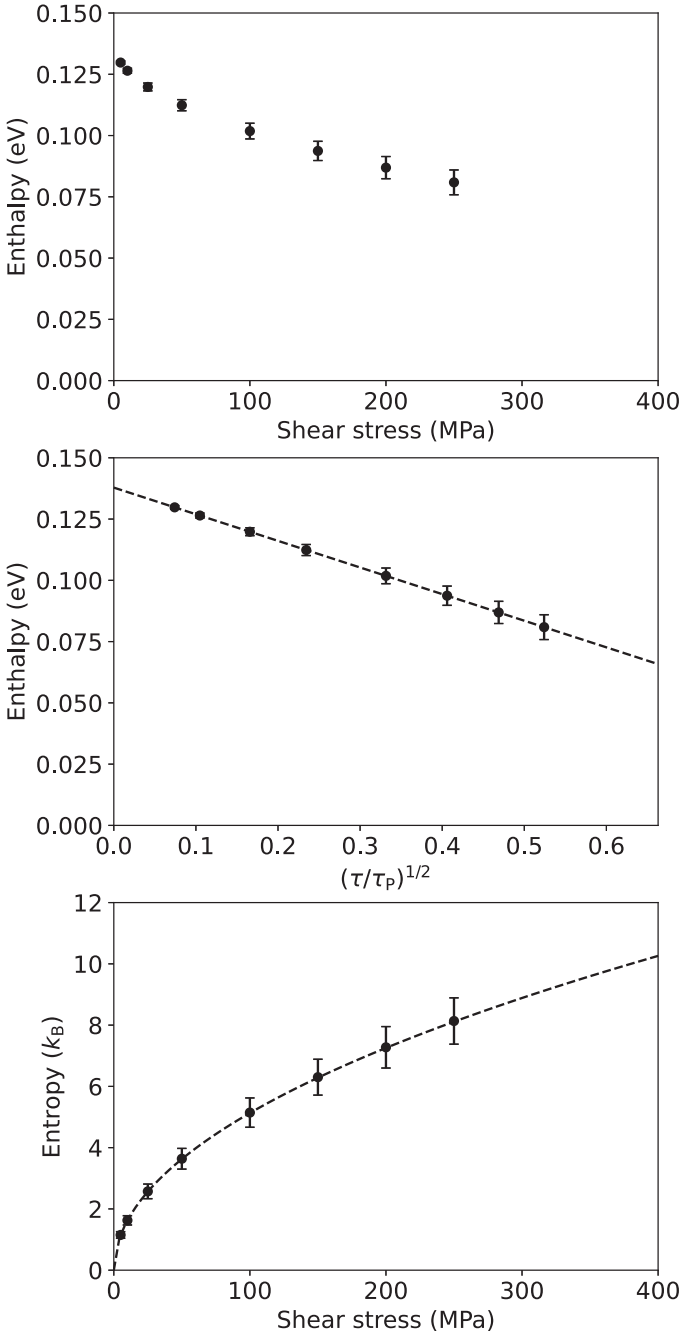

Figure 6. (a) Enthalpy of kink pair formation, $\Delta H_{kp}(\tau)$, as a function of external shear stress τ. (b) $\Delta H_{kp}(\tau)$ fitted with the expression $2H_k - A \cdot \left(\tau/\tau_P\right)^{1/2}$ (dashed line) and plotted as a function of $\left(\tau/\tau_P\right)^{1/2}$. (c) Entropy of kink pair formation, $\Delta S_{kp}(\tau)$, as a function of shear stress. The dashed line in (c) is a fit assuming a square root dependence on τ (see text).

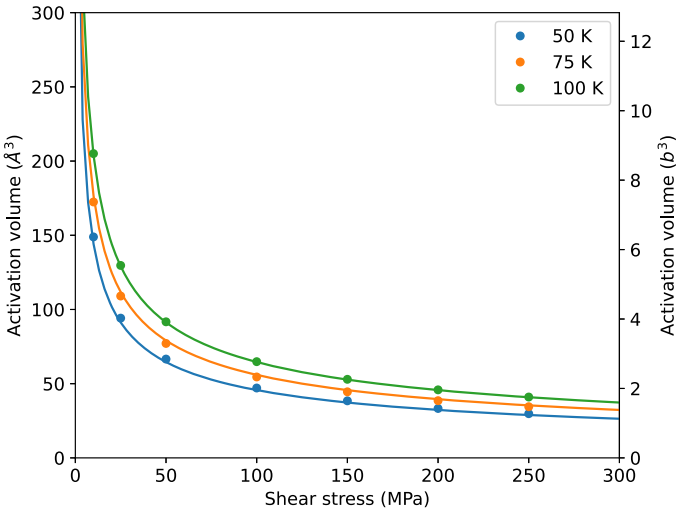

Figure 7. Activation volume as a function of shear stress at different temperatures. The full lines are fits through the data using equation (23).

As shown by the colored solid lines in figure 4, all of the $\Delta G_{\rm kp}$ values can be fitted simultaneously using the empirical model of reference [3]

$$\Delta G_{\rm kp}(\tau, T) = \Delta G_0 \left[1 - \left(\frac{\tau}{\tau_{\rm c}(T)}\right)^p\right]^l, \tag{18}$$

where the critical shear stresses $\tau_{\rm c}(T)$ are obtained from the constant strain-rate calculations (mean values in table 1), $p = 0.5$, $l = 1$, and the fit parameter ΔG_0 is optimized to 0.138 ± 0.007 eV. The adjusted R^2 value of the fit is 0.991. Note that equation (18) can also be used to derive an expression for the critical shear stress as a function of temperature (see equation (6) in reference [36] and references therein), which describes very well the experimental data for bcc Nb [41] with the same fit parameters $p = 0.5$ and $l = 1$.

The ability to fit well all the $\Delta G_{\rm kp}$ data with the same set of model parameters demonstrates the internal consistency of the methodology. Further, the good fit indicates that the same atomistic mechanism, i.e., the kink-pair formation, is responsible for the onset of the dislocation migration, regardless of stress and temperature.

The temperature dependence of $\Delta G_{\rm kp}(\tau, T)$ at different stresses, calculated using equation (18), is shown in figure 5 by the symbols. The dashed lines in figure 5 represent fits of $\Delta G_{\rm kp}(T)$ as a function of temperature using equation (3) at the different stress levels. From the offset and the slope of the fits, the temperature-averaged, stress-dependent enthalpy and the entropy of kink formation can be obtained. The resulting stress dependence of $\Delta H_{\rm kp}(\tau)$ and $\Delta S_{\rm kp}(\tau)$ is shown in figure 6.

The enthalpy of kink pair formation $\Delta H_{\rm kp}(\tau)$ (figure 6(a)) decreases with increasing shear stress in qualitative agreement with the trend observed in previous studies [9, 10, 43–45] performed at different levels of sophistication. In particular, Koizumi *et al* [10] derived the following expression for the enthalpy of kink pair formation at *low* τ: $\Delta H_{\rm kp}(\tau) = 2H_{\rm k} - A \cdot \left(\tau/\tau_{\rm P}\right)^{1/2}$, where $\tau_{\rm P}$ is the Peierls stress, $2H_{\rm k}$ is the energy of two isolated kinks at zero stress and A is a parameter depending on the shape of the Peierls potential, the cut-off radius of the dislocation core and the shear modulus. The $\Delta H_{\rm kp}(\tau)$ data obtained in the present

study can be well fitted with this equation (figure 6(b)) with $2H_k = 0.138 \pm 0.001$ eV and $A = 0.109 \pm 0.006$ eV, which justifies the extrapolation using equation (18). The derived energy of two isolated kinks at zero stress, i.e., $2H_k = 0.138$ eV, is rather low, compared to the experimental results for bcc Nb (0.68 eV [2, 5]). However, this is not caused by the application of the accelerated MD method. The same too low activation enthalpies are also obtained in brute force MD simulations due to the specificity of the atomistic simulations as compared to experiment [7].

The entropy of kink pair formation $\Delta S_{kp}(\tau)$ increases with increasing shear stress (figure 6(c)), similarly to the results for the entropy of high-temperature flow in Zr, obtained by Jonas and Luton [46]. The observed stress dependence of the activation entropy can be qualitatively understood on the atomistic level using the Boltzmann entropy equation

$$\Delta S_{kp}(\tau) = k_B \log\left(W_{kp}(\tau)\right), \tag{19}$$

where the number of microstates W_{kp} is taken as the number of possible sites for the nucleation of a critical kink pair with a critical width w^*. Numerical calculations using a range of Peierls potentials [10, 11] have shown that w^* decreases rapidly with increasing shear stress for relatively small stresses ($\tau/\tau_P < 0.3$). The Peierls stress for the investigated dipole model is about $\tau_P = 910$ MPa and thus the shear stresses τ, considered in figure 6, fall in this range of $\tau/\tau_P < 0.3$. Taking a common formulation $W_{kp} = \tilde{L}/w^*$, where $\tilde{L}$ is the dislocation length [9], it can be seen that both W_{kp} and ΔS_{kp} should be increasing functions of stress.

A phenomenological model for the observed stress-dependence of the entropy can be motivated as follows. The entropy can be written as [3, 46]:

$$\Delta S_{kp}(\tau) = \Delta S_{kp}(\tau = 0) + \int_0^\tau \left(\frac{\partial \Delta S_{kp}}{\partial \tau'}\right)_T \mathrm{d}\tau'. \tag{20}$$

Equation (20) can be transformed, using the Maxwell relation $\left(\partial \Delta S_{kp}/\partial \tau\right)_T = \left(\partial V^*/\partial T\right)_\tau$ and assuming that $\Delta S_{kp}(\tau = 0) = 0$ [17], into:

$$\Delta S_{kp}(\tau) = \int_0^\tau \left(\frac{\partial \Delta V^*}{\partial T}\right)_\tau \mathrm{d}\tau'. \tag{21}$$

The stress dependence of the activation volume V^* can be calculated from the Gibbs energy of kink pair formation equation (18) (with $p = 0.5$ and $l = 1.0$) using equation (6) and it reads

$$V^*(\tau) = \frac{\Delta G_0}{2}\left(\frac{1}{\tau \cdot \tau_c(T)}\right)^{0.5}. \tag{22}$$

Figure 7 exemplifies the stress dependence of V^* for the three investigated temperatures (filled symbols). The activation volume decreases with increasing shear stress in qualitative agreement with experiments [47]. To utilize equation (22) in equation (21), we need an explicit functional dependence of V^* on temperature. Our results (table 1) suggest that in the investigated temperature interval this functional dependence can be approximated by an inverse relation between the temperature and the critical stress τ_c, which implies that the temperature dependence of the activation volume can be approximated as

$$V^*(\tau, T) \approx \frac{\Delta G_0}{2}\left(\frac{\alpha T}{\tau}\right)^n, \tag{23}$$

with $n = 0.5$ and a proportionality constant α. The activation-volume data from all temperatures (all symbols in figure 7) can be very well fitted with equation (23) using α as the

single fitting coefficient as highlighted by the solid colored curves in figure 7 ($\alpha = 3.415 \times 10^{-5}$ (MPa K)$^{-1}$, adjusted $R^2 = 0.9996$). The same stress dependence $V^* \sim \tau^{-1/2}$ is predicted in the framework of the so-called elastic-interaction model [2]. The good fit of the computed activation volume and the consistency with the elastic-interaction model further validates the extrapolation procedure using equation (18).

In the case when $n = 1$ and $\alpha\Delta G_0/2 = k_B m$, equation (23) reduces to the commonly used expression $V^* = k_B T/m\tau$, where m is the strain rate sensitivity. Inserting equation (23) into equation (21) and integrating over τ, a square root dependence on τ is obtained for the entropy

$$\Delta S_{kp}(\tau) \propto \tau^{1/2}. \tag{24}$$

Utilizing this insight and fitting the previously discussed $\Delta S_{kp}(\tau)$ values to a square root dependence, gives an excellent fit as shown in figure 6(c) by the dashed line (adjusted $R^2 = 1$, proportionality coefficient $0.51 \pm 0.02 k_B$ MPa$^{-1/2}$).

The entropy values obtained are larger than the simple vibrational estimate ($\Delta S_{kp} \approx 2/3 k_B$) derived analytically by Friedel [18]. This suggests that the vibrational contribution to the entropy of kink pair formation at low temperatures is smaller than the configurational (elastic) contribution.

The enthalpy decreases (figure 6(a)), while the entropy increases (figure 6(c)) with increasing shear stress. This implies that the thermodynamic data computed here do not follow the empirical Meyer–Neldel rule [48], according to which the entropy is proportional to the enthalpy ($\Delta S = \Delta H/T_{MN}$, where T_{MN} is the Meyer–Neldel temperature). The Meyer–Neldel rule can be derived using standard thermodynamic relations from the following Gibbs activation energy: $\Delta G(\tau, T) = (1 - T/T_{MN})\Delta H(\tau)$. This simple approximation does not describe well the Gibbs energy of kink pair nucleation in bcc metals with a large Peierls barrier like Nb, because it neglects configurational contributions to the entropy and the temperature dependence of the critical shear stress [49]. The Meyer–Neldel rule is observed, for example, during dislocation cross-slip in Al at high temperatures [50] and creep in fcc Cu [30], but not during the dislocation motion through a field of solutes in Al–Mg alloys [49].

4. Conclusions

The Gibbs energy of kink pair formation on screw dislocations in bcc Nb has been computed at different shear stress levels and temperatures using a recently proposed method. This method features a strain reduction procedure that brings the system into mechanical equilibrium at a constant stress level, a situation that is ideally suited to apply acceleration techniques to MD simulations. Thereby, dislocation migration can be studied within accessible simulation times at low temperatures in the thermally-activated regime of kink pair nucleation for stresses below the critical shear stress.

The computed Gibbs energy of kink pair formation increases with both, decreasing shear stress and decreasing temperature. The functional dependence on the shear stress and temperature can be well fitted by an empirical model with only a single set of model parameters. This result demonstrates the consistency of the method and reveals that—for all investigated stresses and temperatures—the same type of kink-pair formation on the screw dislocation is the active atomistic mechanism responsible for the onset of dislocation migration.

From the Gibbs energy dependencies, the corresponding enthalpy and entropy of kink pair formation and the activation volume could be obtained by utilizing standard thermodynamic relations. The activation enthalpy and activation volume decrease with increasing shear stress

in qualitative agreement with phenomenological models proposed in the literature. The activation entropy of kink pair formation is of the order of $2k_B$ at $\tau = 25$ MPa and increases significantly with increasing shear stress. A phenomenological derivation has been provided to motivate the stress dependence of the entropy. The derivation predicts a $\tau^{1/2}$ dependence, which fits well the entropy data obtained in the molecular dynamic simulations.

The utilized strain-reduction approach based on accelerated MD and the global bond-boost potential can be extended to larger supercells, other metals and interatomic potentials. The boost potential does not depend explicitly on the underlying interatomic interactions and it is short-ranged, boosting a single bond at every HD step. Moreover, the formation of critical kink pairs is a localized event, involving only few additional atoms in the dislocation core. Application of *local* HD, in which multiple pairs of atoms are boosted at each time step and which could thereby speed-up the simulations further, is a promising direction for future studies.

Conflict of interest

No potential conflict of interest was reported by the authors

Acknowledgments

This project has received funding from the European Research Council (ERC) under the European Union's Horizon 2020 research and innovation program (Grant Agreement No. 865855). Support by the Stuttgart Center for Simulation Science (SimTech) is gratefully acknowledged. The authors also acknowledge support by the state of Baden-Württemberg through bwHPC and the German Research Foundation (DFG) through Grant No. INST 40/467-1 FUGG (JUSTUS cluster).

Data availability statement

All data that support the findings of this study are included within the article (and any supplementary files).

ORCID iDs

Nikolay Zotov https://orcid.org/0000-0002-6098-4086
Blazej Grabowski https://orcid.org/0000-0003-4281-5665

References

[1] Suzuki T, Kamimura Y and Kirchner H O K 1999 Plastic homology of bcc metals *Phil. Mag.* A **79** 1629
[2] Seeger A 2002 Peierls barriers, kinks, and flow stress: recent progress *Z. Metall.* **93** 760
[3] Kocks U F, Argon A S and Ashby M F 1975 Thermodynamics and kinetics of slip *Progress in Materials Science* ed B ed Chalmers, J W Christian and T B Massalski (Oxford: Pergamon) pp 1–281
[4] Hirth J P and Lothe J 1982 *Theory of Dislocations* (New York: Wiley)
[5] Seeger A and Holzwarth U 2006 Slip planes and kink properties of screw dislocations in high-purity niobium *Phil. Mag.* **86** 3861

[6] Weinberger C R, Boyce B L and Battaile C C 2013 Slip planes in bcc transition metals *Int. Mater. Rev.* **58** 296
[7] Grabowski B and Zotov N 2021 Thermally-activated dislocation mobility in bcc metals: an accelerated molecular dynamics study *Comput. Mater. Sci.* **200** 110804
[8] Ryu S, Kang K and Cai W 2011 Predicting the dislocation nucleation rate as a function of temperature and stress *J. Mater. Res.* **26** 2335
[9] Guyot P and Dorn J E 1967 A critical review of the Peierls mechanism *Can. J. Phys.* **45** 983
[10] Koizumi H, Kirchner H O K and Suzuki T 1993 Kink pair nucleation and critical shear stress *Acta Metall. Mater.* **41** 3483
[11] Koizumi H, Kirchner H O K and Suzuki T 1994 Nucleation of trapezoidal kink pairs on a Peierls potential *Phil. Mag.* A **69** 805
[12] Schoeck G 1965 The activation energy of dislocation movement *Phys. Status Solidi b* **8** 499
[13] Dimelfi R J, Nix W D, Barnett D M, Holbrook J H and Pound G M 1976 An analysis of the entropy of thermally activated dislocation motion based on the theory of thermoelasticity *Phys. Status Solidi b* **75** 573
[14] Schoeck G 1980 The entropy of internal stress fields *Phys. Status Solidi b* **97** 345
[15] Gibbs G B 1965 The thermodynamics of thermally-activated dislocation glide *Phys. Status Solidi b* **10** 507
[16] Surek T, Luton M J and Jonas J J 1973 Dislocation glide controlled by linear elastic obstacles: a thermodynamic analysis *Phil. Mag.* A **27** 425
[17] Burns S J 2018 Elastic shear modulus constitutive law found from entropy considerations *J. Appl. Phys.* **124** 085904
[18] Friedel J 1982 On the entropy of vibration of dislocations *Phil. Mag.* A **45** 271
[19] Granato A V, Lücke K, Schlipf J and Teutonico L J 1964 Entropy factors for thermally activated unpinning of dislocations *J. Appl. Phys.* **35** 2732
[20] Ladd A J C and Hoover W G 1982 Energy and entropy of interacting dislocations *Phys. Rev.* B **26** 5469
[21] Marklund S 1985 The entropy factor involved in the Hirth and Lothe theory of dislocation velocity in silicon *Solid State Commun.* **54** 555
[22] Forsblom M, Sandberg N and Grimvall G 2004 Vibrational entropy of dislocations in Al *Phil. Mag.* **84** 521
[23] Schuck P C, Marian J, Adams J B and Sadigh B 2009 Vibrational properties of straight dislocations in bcc and fcc metals within the harmonic approximation *Phil. Mag.* **89** 2861
[24] Vineyard G H 1957 Frequency factors and isotope effects in solid state rate processes *J. Phys. Chem. Solids* **3** 121
[25] Hirth J P and Nix W D 1969 An analysis of the thermodynamics of dislocation glide *Phys. Status Solidi b* **35** 177
[26] Jin C, Ren W and Xiang Y 2010 Computing transition rates of thermally activated events in dislocation dynamics *Scr. Mater.* **62** 206
[27] Uranagase M and Matsumoto R 2014 Thermal activation analysis of enthalpic and entropic contributions to the activation free energy of basal and prismatic slips in Mg *Phys. Rev.* B **89** 224103
[28] Hara S and Li J 2010 Adaptive strain-boost hyperdynamics simulations of stress-driven atomic processes *Phys. Rev.* B **82** 184114
[29] Ishii A, Ogata S, Kimizuka H and Li J 2012 Adaptive-boost molecular dynamics simulation of carbon diffusion in iron *Phys. Rev.* B **85** 064303
[30] Wang Y-J, Ishii A and Ogata S 2013 Entropic effect on creep in nanocrystalline metals *Acta Mater.* **61** 3866
[31] Du J-P, Wang Y-J, Lo Y-C, Wan L and Ogata S 2016 Mechanism transition and strong temperature dependence of dislocation nucleation from grain boundaries: an accelerated molecular dynamics study *Phys. Rev.* B **94** 104110
[32] Wang Y-J, Du J-P, Shinzato S, Dai L-H and Ogata S 2018 A free energy landscape perspective on the nature of collective diffusion in amorphous solids *Acta Mater.* **157** 165
[33] Yang Y-B, Yang Q, Wei D, Dai L-H, Yu H-B and Wang Y-J 2020 Unraveling strongly entropic effect on β-relaxation in metallic glass: insights from enhanced atomistic samplings over experimentally relevant timescales *Phys. Rev.* B **102** 174103
[34] Plimpton S 1995 Fast parallel algorithms for short-range molecular dynamics *J. Comput. Phys.* **117** 1

[35] Farkas D and Jones C 1996 Interatomic potentials for ternary Nb–Ti–Al alloys *Modelling Simul. Mater. Sci. Eng.* **4** 23
[36] Zotov N and Grabowski B 2021 Molecular dynamics simulations of screw dislocation mobility in bcc Nb *Modelling Simul. Mater. Sci. Eng.* **29** 085007
[37] Hirel P 2015 Atomsk: a tool for manipulating and converting atomic data files *Comput. Phys. Commun.* **197** 212
[38] Gilbert M R, Queyreau S and Marian J 2011 Stress and temperature dependence of screw dislocation mobility in α-Fe by molecular dynamics *Phys. Rev.* B **84** 174103
[39] Stukowski A 2009 Visualization and analysis of atomistic simulation data with OVITO—the open visualization tool *Modelling Simul. Mater. Sci. Eng.* **18** 015012
[40] Voter A F 1997 A method for accelerating the molecular dynamics simulation of infrequent events *J. Chem. Phys.* **106** 4665
[41] Takeuchi S, Hashimoto T and Maeda K 1982 Plastic deformation of bcc metal single crystals at very low temperatures *Trans. Japan Inst. Met.* **23** 60
[42] Huang C, Perez D and Voter A F 2015 Hyperdynamics boost factor achievable with an ideal bias potential *J. Chem. Phys.* **143** 074113
[43] Itakura M, Kaburaki H and Yamaguchi M 2012 First-principles study on the mobility of screw dislocations in bcc iron *Acta Mater.* **60** 3698
[44] Dezerald L, Proville L, Ventelon L, Willaime F and Rodney D 2015 First-principles prediction of kink-pair activation enthalpy on screw dislocations in bcc transition metals: V, Nb, Ta, Mo, W, and Fe *Phys. Rev.* B **91** 094105
[45] Maresca F, Dragoni D, Csányi G, Marzari N and Curtin W A 2018 Screw dislocation structure and mobility in body centered cubic Fe predicted by a Gaussian approximation potential *npj Comput. Mater.* **4** 69
[46] Jonas J J and Luton M J 1971 The activation entropy of high temperature flow *Metall. Mater. Trans.* B **2** 3492
[47] Croteau J-F *et al* 2020 Effect of strain rate on tensile mechanical properties of high-purity niobium single crystals for SRF applications *Mater. Sci. Eng.* A **797** 140258
[48] Meyer W and Neldel H 1937 Concerning the relationship between the energy constant epsilon and the quantum constant alpha in the conduction-temperature formula in oxidising semi-conductors *Phys. Z.* **38** 1014
[49] Saroukhani S and Warner D H 2017 Investigating dislocation motion through a field of solutes with atomistic simulations and reaction rate theory *Acta Mater.* **128** 77
[50] Esteban-Manzanares G, Santos-Güemes R, Papadimitriou I, Martínez E and LLorca J 2020 Influence of the stress state on the cross-slip free energy barrier in Al: an atomistic investigation *Acta Mater.* **184** 109